

# Higgs- $\mu$ - $\tau$ Coupling at High and Low Energy Colliders

Ying-nan Mao <sup>1</sup> and Shou-hua Zhu <sup>1,2,3</sup>

<sup>1</sup> *Institute of Theoretical Physics & State Key Laboratory of Nuclear Physics and Technology,*

*Peking University, Beijing 100871, China*

<sup>2</sup> *Collaborative Innovation Center of Quantum Matter, Beijing 100871, China*

<sup>3</sup> *Center for High Energy Physics, Peking University, Beijing 100871, China*

(Dated: April 25, 2022)

There is no tree-level flavor changing neutral current (FCNC) in the standard model (SM) which contains only one Higgs doublet. If more Higgs doublets are introduced for various reasons, the tree level FCNC would be inevitable except extra symmetry was imposed. Therefore FCNC processes are the excellent probes for the physics beyond the SM (BSM). In this paper, we studied the lepton flavor violated (LFV) decay processes  $h \rightarrow \mu\tau$  and  $\tau \rightarrow \mu\gamma$  induced by Higgs- $\mu$ - $\tau$  vertex. For  $\tau \rightarrow \mu\gamma$ , its branching ratio is also related to the  $h\bar{t}t$ ,  $h\tau^+\tau^-$  and  $hW^+W^-$  vertices. We categorized the BSM into two scenarios for the Higgs coupling strengths near or away from SM. For the latter scenario, we took the spontaneously broken two Higgs doublet model (Lee model) as an example. We considered the constraints by recent data from LHC and B factories, and found that the measurements gave weak constraints. At LHC Run II,  $h \rightarrow \mu\tau$  will be confirmed or set stricter limit on its branching ratio. Accordingly,  $\text{Br}(\tau \rightarrow \mu\gamma) \lesssim \mathcal{O}(10^{-10} - 10^{-8})$  for general chosen parameters. For the positive case,  $\tau \rightarrow \mu\gamma$  can be discovered with  $\mathcal{O}(10^{10})$   $\tau$  pair samples at SuperB factory, Super  $\tau$ -charm factory and new Z-factory. The future measurements for  $\text{Br}(h \rightarrow \mu\tau)$  and  $\text{Br}(\tau \rightarrow \mu\gamma)$  will be used to distinguish these two scenarios or set strict constraints on the correlations among different Higgs couplings, please see Table II in the text for details.

## I. INTRODUCTION

In the standard model (SM), we can diagonalize the gauge couplings and Yukawa couplings simultaneously, i.e., there is no flavor changing neutral current (FCNC) at the tree level. In the quark sector, flavor changing neutral currents occur at loop level with the help of CKM quark mixing matrix [1]. However, in the lepton sector, it is extremely suppressed by GIM mechanism [2] in the SM due to the smallness of neutrino mass. For example, for the lepton flavor violation (LFV) process  $\ell_i \rightarrow \ell_j \gamma$

$$\frac{\Gamma(\ell_i \rightarrow \ell_j \gamma)}{\Gamma(\ell_i \rightarrow \ell_j \nu_i \bar{\nu}_j)} = \frac{3\alpha}{32\pi} \left| \sum_k V_{ik}^* V_{jk} \frac{m_{\nu_k}^2}{m_W^2} \right|^2 \quad (1)$$

in the SM [3] where  $V_{ij}$  are the PMNS lepton mixing matrix [4] elements. With the data from neutrino oscillation [5], it is estimated to be

$$\text{Br}(\mu \rightarrow e \gamma) \sim \mathcal{O}(10^{-56}) \quad \text{and} \quad \text{Br}(\tau \rightarrow e(\mu) \gamma) \sim \mathcal{O}(10^{-55} - 10^{-54}) \quad (2)$$

in the SM. It is far away from the recent experimental upper limit [6, 7]<sup>1</sup>

$$\begin{aligned} \text{Br}(\tau \rightarrow e \gamma) &< \begin{cases} 1.2 \times 10^{-7} & (\text{Belle}) \\ 3.3 \times 10^{-8} & (\text{BaBar}) \end{cases}, \quad \text{Br}(\tau \rightarrow \mu \gamma) < \begin{cases} 4.5 \times 10^{-8} & (\text{Belle}) \\ 4.4 \times 10^{-8} & (\text{BaBar}) \end{cases}, \\ \text{and } \text{Br}(\mu \rightarrow e \gamma) &< 5.7 \times 10^{-13} \quad (\text{MEG}), \quad \text{all at 90\% C.L.} \end{aligned} \quad (3)$$

and the near future sensitivities with the improvement of an order [8–11]. So that the discovery of the signals  $\ell_i \rightarrow \ell_j \gamma$  at future colliders would clearly indicate new physics (NP) beyond the SM (BSM). Generally speaking the FCNC process will be one of the best probe of the BSM for future hadron and electron-positron colliders [12].

In July 2012, a new boson was discovered at LHC [13, 14], and its properties are like those of a SM Higgs boson [15]. The Higgs mediated LFV process is attractive because of a  $2.4\sigma$  hint found by CMS Collaboration [16] in the search for  $h \rightarrow \mu\tau$  process<sup>2</sup>. Assuming that the Higgs production cross section and total decay width are the same as those in the SM, the best fit (B.F.) branching ratio and 95% upper limit (U.L.) are respectively [16]<sup>3</sup>

$$\text{Br}(h \rightarrow \mu\tau) = (0.84_{-0.37}^{+0.39})\% \quad (\text{B.F.}) \quad \text{and} \quad \text{Br}(h \rightarrow \mu\tau) < 1.51\% \quad (\text{U.L.}) \quad (4)$$

<sup>1</sup> For either B factory with  $L \approx 0.5 \text{ ab}^{-1}$  luminosity at  $\sqrt{s} = 10.6 \text{ GeV}$  ( $\Upsilon(4S)$  threshold).

<sup>2</sup> Recently the ATLAS Collaboration also published the searching result in the same process [17] with the result close to that in [16] by CMS Collaboration.

<sup>3</sup> For the full LHC Run I data with  $L \approx 25 \text{ fb}^{-1}$  luminosity at  $\sqrt{s} = (7-8) \text{ TeV}$ .

If this signature was confirmed at future colliders, it would clearly indicate NP in the Higgs sector. In the extensions of SM, there may be direct Higgs- $\mu$ - $\tau$  coupling to explain this hint, for example, in some types of two Higgs doublet models (2HDM) [18], like type III 2HDM [19–22], 2HDMs with other flavor symmetries [23–25], Lee model [26, 27], and other models [28–30]. It may be also related to other phenomena like the excess in  $t\bar{t}h$  searches [31],  $b \rightarrow s$  semi-leptonic decays [24], anomalous magnetic moment ( $g - 2$ ) for  $\mu$  [32], LFV  $\tau$  decays [21, 25, 32–34], or even the lepton flavored dark matter [35]. Writing the Higgs- $\mu$ - $\tau$  vertex as

$$\mathcal{L}_{h\mu\tau} = -\frac{h}{\sqrt{2}} (Y_{\mu\tau}\bar{\mu}_L\tau_R + Y_{\tau\mu}\bar{\tau}_L\mu_R + \text{h.c.}), \quad (5)$$

and adopting the Cheng-Sher ansatz [36], the data gave [16]

$$\sqrt{|Y_{\mu\tau}|^2 + |Y_{\tau\mu}|^2} < 5 \times 10^{-3} \quad \text{or} \quad \sqrt{\frac{(|Y_{\mu\tau}|^2 + |Y_{\tau\mu}|^2)v^2}{2m_\mu m_\tau}} < 2. \quad (6)$$

In the future, at low energy  $e^+e^-$  colliders like Super-B factory [9, 10], Super  $\tau$ -charm factory [37, 38] or the new Z-factory [39], there would be signatures or stricter constraints for  $\tau \rightarrow \mu\gamma$  process; and at high energy colliders like LHC Run II at  $\sqrt{s} = (13 - 14)\text{TeV}$ , there would be signatures or stricter constraints for  $h \rightarrow \mu\tau$  process. The results would be comparable and may give new constraints on the Higgs- $\mu$ - $\tau$  coupling or the correlations among the couplings between Higgs and other particles.

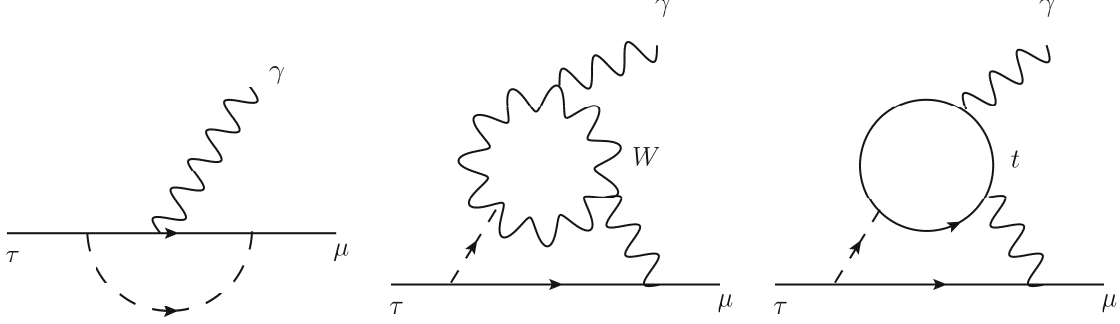
This paper is organized as follows. In section II we present the effective interactions and branching ratios for  $h \rightarrow \mu\tau$  and  $\tau \rightarrow \mu\gamma$  processes; section III and section IV contain the constraints from recent data and at future colliders respectively; section V are our conclusions and discussions.

## II. EFFECTIVE HIGGS- $\mu$ - $\tau$ INTERACTION AND DECAY WIDTHS FOR $h \rightarrow \mu\tau$ AND $\tau \rightarrow \mu\gamma$ PROCESSES

Based on 2HDM (type III), the higgs effective couplings can be written as

$$\begin{aligned} \mathcal{L}_h = & c_V h \left( \frac{2m_W^2}{v} W^{+\mu} W_\mu^- + \frac{m_Z^2}{v} Z^\mu Z_\mu \right) - h \left( \frac{c_t m_t}{v} \bar{t}_L t_R + \frac{c_\tau m_\tau}{v} \bar{\tau}_L \tau_R + \text{h.c.} \right) \\ & - \frac{h}{\sqrt{2}} (Y_{\mu\tau}\bar{\mu}_L\tau_R + Y_{\tau\mu}\bar{\tau}_L\mu_R + \text{h.c.}) \end{aligned} \quad (7)$$

FIG. 1: Typical Feynman diagrams which contribute to  $\tau \rightarrow \mu\gamma$  decay. The left one is Higgs-mediated one-loop diagram, the middle and right ones are  $W$  boson and top quark mediated Barr-Zee Type two-loop diagrams respectively.



where  $c_i$  stands for the coupling strength ratio compared with that in SM<sup>4</sup> and  $Y_{ij}$  stands for the LFV coupling just like that in Eq. (5). With a direct calculation [16], for the  $h \rightarrow \mu\tau$  process, we have

$$\text{Br}(h \rightarrow \mu\tau) = \frac{m_h}{16\pi\Gamma_h} (|Y_{\mu\tau}|^2 + |Y_{\tau\mu}|^2) \quad (8)$$

where  $\Gamma_h$  means the total decay width of Higgs boson and in SM we have  $\Gamma_{h,\text{SM}} = 4.1\text{MeV}$  [40] for  $m_h = 125\text{GeV}$ .

The  $\tau \rightarrow \mu\gamma$  decay process is loop induced. The dominant contribution usually comes from Barr-Zee type<sup>5</sup> two-loop diagrams since there is an additional  $(m_\tau/m_h)^2 \log(m_h^2/m_\tau^2) \sim \mathcal{O}(10^{-3})$  suppression in the one-loop amplitude [42], see the Feynman diagrams in Figure 1. Following the formulae in [42],

$$\frac{\text{Br}(\tau \rightarrow \mu\gamma)}{\text{Br}(\tau \rightarrow \mu\nu\bar{\nu})} = \frac{48\pi^3\alpha}{G_F^2} (|\mathcal{A}_L|^2 + |\mathcal{A}_R|^2). \quad (9)$$

<sup>4</sup> The  $c_t$  and  $c_\tau$  may be complex while  $c_V$  must be real, and in the SM  $c_V = c_t = c_\tau = 1$ .

<sup>5</sup> This type of two-loop diagrams was first proposed by Barr and Zee [41] during the calculation for lepton electric dipole moment (EDM).

Here the left (right) handed amplitudes  $\mathcal{A}_{L(R)}$  can be expressed as [20, 32, 42, 43]<sup>6</sup>

$$\begin{aligned}
& \mathcal{A}_L(\mathcal{A}_R^*) \\
&= \mathcal{A}_{L,1\text{-loop}}(\mathcal{A}_{R,1\text{-loop}}^*) + \mathcal{A}_{L,2\text{-loop}}(\mathcal{A}_{R,2\text{-loop}}^*) \\
&= \frac{Y_{\mu\tau}(Y_{\tau\mu}^*)}{16\sqrt{2}\pi^2} \left( \frac{m_\tau}{m_h^2 v} \left( c_\tau \ln \left( \frac{m_h^2}{m_\tau^2} \right) - \frac{4}{3} \text{Re}(c_\tau) - \frac{5i}{3} \text{Im}(c_\tau) \right) \right. \\
&\quad + \frac{c_V \alpha}{\pi m_\tau v} \left( \left( 3 + \frac{m_h^2}{2m_W^2} \right) f \left( \frac{m_W^2}{m_h^2} \right) + \left( \frac{23}{4} - \frac{m_h^2}{2m_W^2} \right) g \left( \frac{m_W^2}{m_h^2} \right) + \frac{3}{4} h \left( \frac{m_W^2}{m_h^2} \right) \right) \\
&\quad \left. - \frac{8\alpha}{3\pi m_\tau v} \left( \text{Re}(c_t) f \left( \frac{m_t^2}{m_h^2} \right) + i \text{Im}(c_t) g \left( \frac{m_t^2}{m_h^2} \right) \right) \right) \tag{10}
\end{aligned}$$

where all the functions  $f, g$  and  $h$  come from 2-loop integrations as [43]

$$f(z) = \frac{z}{2} \int_0^1 dx \frac{1-2x(1-x)}{x(1-x)-z} \ln \left( \frac{x(1-x)}{z} \right); \tag{11}$$

$$g(z) = \frac{z}{2} \int_0^1 dx \frac{1}{x(1-x)-z} \ln \left( \frac{x(1-x)}{z} \right); \tag{12}$$

$$h(z) = -\frac{z}{2} \int_0^1 dx \frac{1}{x(1-x)-z} \left( 1 - \frac{z}{x(1-x)-z} \ln \left( \frac{x(1-x)}{z} \right) \right). \tag{13}$$

The small contributions from heavy neutral higgses, charged higgs and  $Z$ -mediated loop are all ignored. Defining

$$\mathcal{A} \equiv \frac{\mathcal{A}_L}{Y_{\mu\tau}} = \frac{\mathcal{A}_R}{Y_{\tau\mu}}, \tag{14}$$

the equation (9) should be changed to

$$\frac{\text{Br}(\tau \rightarrow \mu\gamma)}{\text{Br}(\tau \rightarrow \mu\nu\bar{\nu})} = \frac{48\pi^3\alpha|\mathcal{A}|^2}{G_F^2} (|Y_{\mu\tau}|^2 + |Y_{\tau\mu}|^2). \tag{15}$$

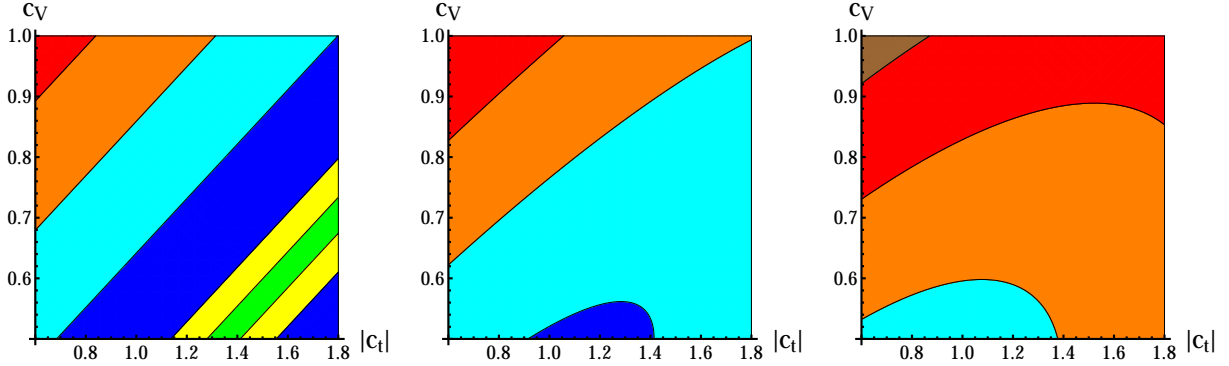
Here  $\text{Br}(\tau \rightarrow \mu\nu\bar{\nu}) = 17.4\%$  from PDG [5].

For both decay processes, the LFV parameter comes in the form  $\sqrt{|Y_{\mu\tau}|^2 + |Y_{\tau\mu}|^2}$ , thus we do not need to study the details about the chiral properties of the LFV coupling. Since both  $\text{Br} \propto (|Y_{\mu\tau}|^2 + |Y_{\tau\mu}|^2)$ , the ratio  $\text{Br}(\tau \rightarrow \mu\gamma)/\text{Br}(h \rightarrow \mu\tau)$  does not depend on  $Y_{\mu\tau(\tau\mu)}$ . Therefore in this paper we will focus on the correlations among the Higgs couplings.

---

<sup>6</sup> The results in these papers are different. We checked the calculations and got the result consistent with that in [32] by Omura et. al.

FIG. 2: Distribution for  $R \equiv \text{Br}(\tau \rightarrow \mu\gamma)/\text{Br}(h \rightarrow \mu\tau)$  in  $c_V - |c_t|$  plane in unit of  $(\Gamma_{h,\text{tot}})/\text{MeV}$  fixing  $c_\tau = 1$ . We take  $\alpha_t = (0, \pi/10, \pi/6)$  from left to right. The green regions are for  $R < 10^{-10}$ ; the yellow regions are for  $10^{-10} \leq R < 10^{-9}$ ; the blue regions are for  $10^{-9} \leq R < 10^{-8}$ ; the cyan regions are for  $10^{-8} \leq R < 3 \times 10^{-8}$ ; the orange regions are for  $3 \times 10^{-8} \leq R < 6 \times 10^{-8}$ ; the red regions are for  $6 \times 10^{-8} \leq R < 10^{-7}$ ; and the brown regions are for  $10^{-7} \leq R < 1.5 \times 10^{-7}$ .



### III. CONSTRAINTS BY RECENT EXPERIMENTS

In general cases,  $\alpha_t \equiv \arg(c_t)$  and  $\alpha_\tau \equiv \arg(c_\tau)$  may be nonzero. The replacement

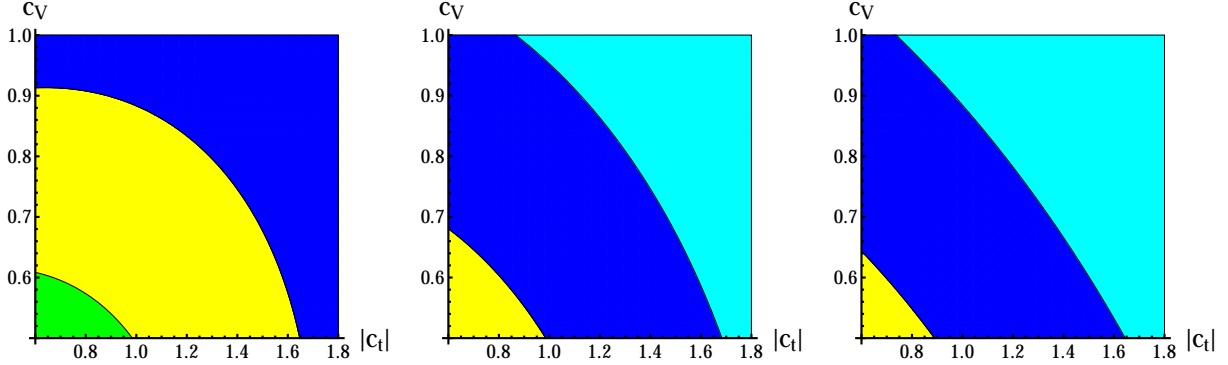
$$\text{Br}(h \rightarrow \mu\tau) \rightarrow \frac{\sigma_h}{\sigma_{h,\text{SM}}} \text{Br}(h \rightarrow \mu\tau) = (\cos^2 \alpha_t + 2.31 \sin^2 \alpha_t) \text{Br}(h \rightarrow \mu\tau) \quad (16)$$

should also be taken into account in (4) where  $\sigma_h$  stands for the Higgs production cross section<sup>7</sup> and  $\sigma_{h,\text{SM}}$  means that in SM. To consider the numerical constraints on the couplings in (7), we should take some benchmark points. Our fitting results [26] preferred  $|c_\tau| \sim 1$  for almost all chosen for other parameters, so in this paper we take  $|c_\tau| = 1$ . The regions  $c_V \lesssim 0.4$ ,  $|c_t| \lesssim 0.5$  and  $|c_t| \gtrsim 2$  are excluded for most cases by our fitting results, so we never consider those regions in this paper.

According to (10),  $R \equiv \text{Br}(\tau \rightarrow \mu\gamma)/\text{Br}(h \rightarrow \mu\tau)$  is sensitive to the interplay between  $c_V$  and  $c_t$ . The cancelation between  $W$  loop and  $t$  loop induced amplitudes would make  $R$  very small in some regions especially for  $\alpha_t \sim 0$ . In Figure 2 and Figure 3, we show some  $R \equiv \text{Br}(\tau \rightarrow \mu\gamma)/\text{Br}(h \rightarrow \mu\tau)$  distribution in  $c_V - |c_t|$  plane in unit of  $(\Gamma_{h,\text{tot}})/\text{MeV}$  for some different  $\alpha_t$ . From the figures, we can also see the cancelation behavior clearly when  $\alpha_t$  is small. For larger  $\alpha_t$ , the imaginary parts of the amplitudes would give more important contributions, and the imaginary parts of one loop contribution would also become more

<sup>7</sup> Gluon fusion process is dominant in this case.

FIG. 3: Distribution for  $R \equiv \text{Br}(\tau \rightarrow \mu\gamma)/\text{Br}(h \rightarrow \mu\tau)$  in  $c_V - |c_t|$  plane in unit of  $(\Gamma_{h,\text{tot}})/\text{MeV}$  fixing  $c_\tau = 1$ . We take  $\alpha_t = (\pi/4, \pi/2, 2\pi/3)$  from left to right. The green regions are for  $R < 10^{-7}$ ; the yellow regions are for  $10^{-7} \leq R < 2 \times 10^{-7}$ ; the blue regions are for  $2 \times 10^{-7} \leq R < 4 \times 10^{-7}$ ; and the cyan regions are for  $4 \times 10^{-7} \leq R < \times 10^{-6}$ .



important as later figures shown.

Here and in the following sections, we categorize BSM into two scenarios. In scenario I, we choose most Higgs couplings close to those in SM, especially  $c_V \sim 1$  and  $\Gamma_h/\Gamma_{h,\text{SM}}$ . Since the experimental data [15] are consistent with the SM predictions, this scenario is popular. While the data still allow the Higgs couplings away from those in SM and these scenarios are attractive, because they are strongly related to BSM physics. In scenario II, we choose Lee model [26, 27] as such a benchmark model. Our previous work [26] showed that there is no SM limit for the lightest scalar in Lee model. We take the 125 GeV Higgs boson as the lightest one, so some of its couplings must be away from those in SM, especially  $c_V$  should be small. In that paper, we considered full constraints by data and showed it is still alive. The fitting results for Higgs signal strengths allowed  $c_V \sim 0.5$ , and at the same time,  $|c_b|$  and  $\Gamma_h$  must be smaller than those in SM. The results are not sensitive to charged Higgs loop contribution. The typical  $\Gamma_h/\Gamma_{h,\text{SM}} \sim \mathcal{O}(0.1)$  for different  $|c_b|$  choice. In both scenarios,  $|c_t| \sim |c_\tau| \sim 1$  are preferred.

In the scenario I, we take  $|c_t| = 0.6, 1.2, 1.8$  and plot the predicted branching ratios for  $\tau \rightarrow \mu\gamma$  in Figure 4 with  $c_V = \Gamma_h/\Gamma_{h,\text{SM}} = 1$  assuming  $\text{Br}(h \rightarrow \mu\tau) = 1.51\%$  as the CMS upper limit, white regions are already excluded by recent data. For  $|c_t| < 1.7$ , all the choices for  $(\alpha_t, \alpha_\tau)$  are still allowed by recent data using this set of benchmark point, thus the recent  $\tau \rightarrow \mu\gamma$  measurements cannot give further constraints. While in the scenario II, the predicted branching ratios for  $\tau \rightarrow \mu\gamma$  are highly suppressed to be of  $\mathcal{O}(10^{-9})$  that

FIG. 4:  $\text{Br}(\tau \rightarrow \mu\gamma)$  distributions in  $\alpha_t - \alpha_\tau$  plane for  $c_V = \Gamma_h/\Gamma_{h,\text{SM}} = 1$ , taking  $|c_t| = 0.6, 1.2, 1.8$  from left to right. The green regions are for  $\text{Br}(\tau \rightarrow \mu\gamma) < 1.5 \times 10^{-8}$ , the yellow regions are for  $1.5 \times 10^{-8} \leq \text{Br}(\tau \rightarrow \mu\gamma) < 3.0 \times 10^{-8}$ , and the blue regions are for  $3.0 \times 10^{-8} \leq \text{Br}(\tau \rightarrow \mu\gamma) < 4.5 \times 10^{-8}$ . White regions are already excluded by recent data.

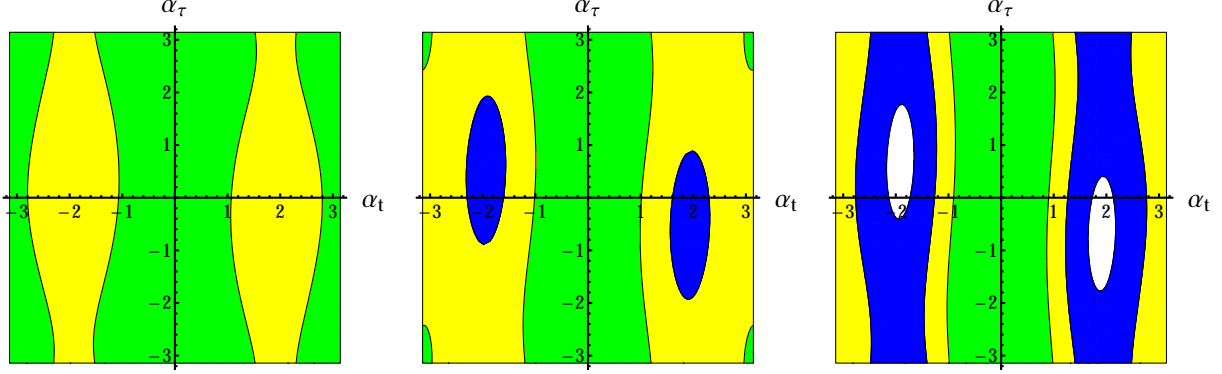
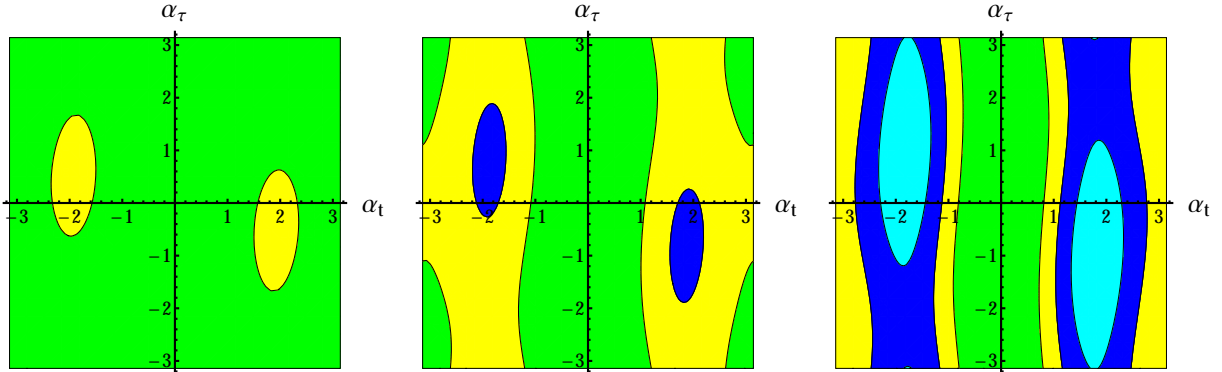


FIG. 5:  $\text{Br}(\tau \rightarrow \mu\gamma)$  distributions in  $\alpha_t - \alpha_\tau$  plane for  $c_V = 0.5$ ,  $\Gamma_h/\Gamma_{h,\text{SM}} = 0.3$ , taking  $|c_t| = 0.6, 1.2, 1.8$  from left to right. The green regions are for  $\text{Br}(\tau \rightarrow \mu\gamma) < 2.5 \times 10^{-9}$ , the yellow regions are for  $2.5 \times 10^{-9} \leq \text{Br}(\tau \rightarrow \mu\gamma) < 5 \times 10^{-9}$ , the blue regions are for  $5 \times 10^{-9} \leq \text{Br}(\tau \rightarrow \mu\gamma) < 7.5 \times 10^{-9}$ , and the cyan regions are for  $7.5 \times 10^{-9} \leq \text{Br}(\tau \rightarrow \mu\gamma) < 1 \times 10^{-8}$ .



Lee model is not constrained by recent data. We take  $|c_t| = 0.6, 1.2, 1.8$  again and plot the predicted  $\text{Br}(\tau \rightarrow \mu\gamma)$  in Lee model in Figure 5 with  $c_V = 0.5$  and  $\Gamma_h/\Gamma_{h,\text{SM}} = 0.3$ , assuming  $\text{Br}(h \rightarrow \mu\tau) = 1.51\%$  as the CMS upper limit.

#### IV. CONSTRAINTS AT FUTURE COLLIDERS

Kopp and Nardecchia [44] studied the phenomenology of  $h \rightarrow \mu\tau$  at future LHC ( $\sqrt{s} = 13\text{TeV}$ ). With  $300\text{fb}^{-1}$  luminosity, their results showed that for  $\sigma_h = \sigma_{h,\text{SM}}$ , if no signal is



observed, the expected upper limit at 95% C.L. should be set as  $\text{Br}(h \rightarrow \mu\tau) < 7.7 \times 10^{-4}$  [44] which means

$$\sqrt{|Y_{\mu\tau}|^2 + |Y_{\tau\mu}|^2} < 1.1 \times 10^{-3} \quad \text{or} \quad \sqrt{\frac{(|Y_{\mu\tau}|^2 + |Y_{\tau\mu}|^2)v^2}{2m_\mu m_\tau}} < 0.45. \quad (17)$$

On the other hand, a signal would be observed at over  $3\sigma$  if  $\text{Br}(h \rightarrow \mu\tau) > 1.3 \times 10^{-3}$  which means

$$\sqrt{|Y_{\mu\tau}|^2 + |Y_{\tau\mu}|^2} > 1.5 \times 10^{-3} \quad \text{or} \quad \sqrt{\frac{(|Y_{\mu\tau}|^2 + |Y_{\tau\mu}|^2)v^2}{2m_\mu m_\tau}} > 0.59. \quad (18)$$

The SuperB factory is a  $e^+e^-$  collider at  $\Upsilon(4S)$  threshold with the luminosity  $75\text{ab}^{-1}$ . For the LFV decay  $\tau \rightarrow \mu\gamma$ , if no signal was observed at the SuperB factory, the expected upper limit at 90% C.L. should be set as [10]

$$\text{Br}(\tau \rightarrow \mu\gamma) < 2.4 \times 10^{-9}. \quad (19)$$

On the other hand, a signal would be observed at over  $3\sigma$  if

$$\text{Br}(\tau \rightarrow \mu\gamma) > 5.4 \times 10^{-9}. \quad (20)$$

At the Super  $\tau$ -charm factory, which is a  $e^+e^-$  collider at  $\sqrt{s} = (2 - 7)\text{GeV}$  with the luminosity  $10\text{ab}^{-1}$ , there would be about  $2.5 \times 10^{10}$  pairs of  $\tau^+\tau^-$  [38]. And the sensitivity for LFV decay  $\tau \rightarrow \mu\gamma$  would be of  $\mathcal{O}(10^{-10})$  [38] because of the suppression in background compared with that at SuperB factory<sup>8</sup>. And the same sensitivity ( $\sim \mathcal{O}(10^{-10})$ ) would be also achieved at new Z-factory [39] with  $\mathcal{O}(10^{12})$  Z bosons.

For the  $\tau \rightarrow \mu\gamma$  results, there are three typical cases listed in Table I in which a positive result means a over  $3\sigma$  evidence and a negative result means an exclusion at 90% C.L. as usual. The typical choices are  $\text{Br}(\tau \rightarrow \mu\gamma) \sim 10^{-8}, 10^{-9}, 10^{-10}$  for each case. And for  $h \rightarrow \mu\tau$

TABLE I: Choices for typical  $\text{Br}(\tau \rightarrow \mu\gamma)$  in different cases.

---

<sup>8</sup> The dominant backgrounds come from  $\tau^+\tau^-\gamma$  events with a hard enough photon at SuperB factory; while at Super  $\tau$ -charm factory,  $\sqrt{s}$  is not far away above the  $\tau^+\tau^-$  threshold that almost all photons from  $\tau^+\tau^-\gamma$  are soft.

	Result at SuperB	Result at Super $\tau$ -charm	Typical choice on $\text{Br}(\tau \rightarrow \mu\gamma)$
Case I	Positive	Positive	$\sim 10^{-8}$
Case II	Negative	Positive	$\sim 10^{-9}$
Case III	Negative	Negative	$\lesssim 2 \times 10^{-10}$

results, we should consider the cases for LHC with positive or negative result separately.

### A. LHC with Positive Result

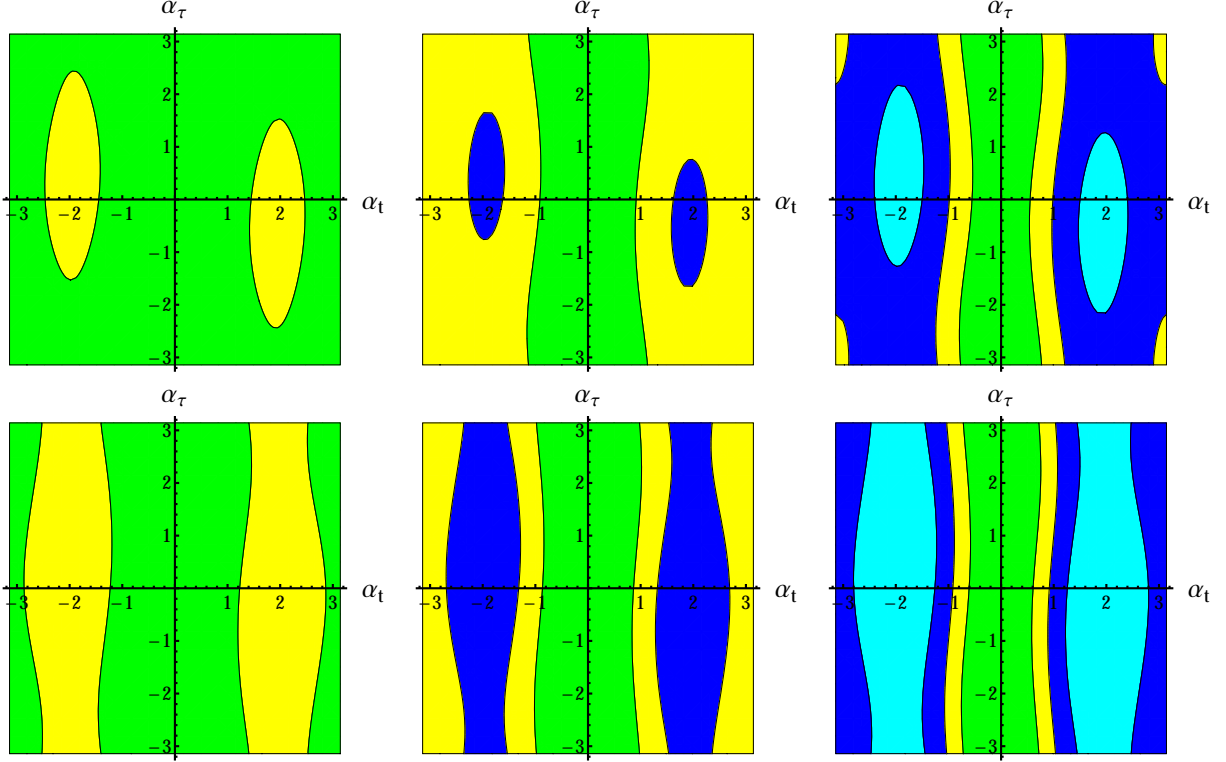
A positive result in the  $h \rightarrow \mu\tau$  search would mean a direct evidence on LFV Higgs- $\mu$ - $\tau$  coupling. We take  $(\sigma_h/\sigma_{h,\text{SM}})\text{Br}(h \rightarrow \mu\tau) = 1.5 \times 10^{-3}$ ,  $3 \times 10^{-3}$ , and  $6 \times 10^{-3}$  as benchmark points in this subsection.

First, consider scenario I in section III where the coupling strengths are close to those in the SM. Taking  $c_V = \Gamma_h/\Gamma_{h,\text{SM}} = 1$ ,  $|c_t| = 1$  and 1.5, we show the  $\text{Br}(\tau \rightarrow \mu\gamma)$  distributions in  $\alpha_t - \alpha_\tau$  plane in Figure 6 with the boundaries set according to the sensitivity of SuperB factory. We can see that if  $(\sigma_h/\sigma_{h,\text{SM}})\text{Br}(h \rightarrow \mu\tau) \gtrsim (2 - 3) \times 10^{-3}$ , the typical predicted  $\text{Br}(\tau \rightarrow \mu\gamma)$  would reach the SuperB sensitivity. While if  $(\sigma_h/\sigma_{h,\text{SM}})\text{Br}(h \rightarrow \mu\tau)$  was smaller, the  $\tau \rightarrow \mu\gamma$  process would not be found at SuperB factory.

Then we should focus on the green regions which mean the cases with negative results at SuperB factory. Here we show the  $\text{Br}(\tau \rightarrow \mu\gamma)$  distributions in  $\alpha_t - \alpha_\tau$  plane in Figure 7 with the boundaries set according to the sensitivity of Super  $\tau$ -charm factory. For  $\text{Br}(\tau \rightarrow \mu\gamma) \sim 10^{-9}$  or smaller,  $|\alpha_t| \lesssim 1.5$  were favored. If LHC gave positive results, the typical predicted  $\text{Br}(\tau \rightarrow \mu\gamma)$  must reach the sensitivity of Super  $\tau$ -charm factory in this scenario. If Super  $\tau$ -charm factory gave negative results, it would give strict constraints on the Higgs couplings.

In summary, For case I in Table I, if the SuperB factory gave positive results in searching  $\tau \rightarrow \mu\gamma$  (thus it must be discovered at Super  $\tau$ -charm factory as well),  $(\alpha_t, \alpha_\tau)$  would fall into the blue or cyan regions in Figure 6. The value of  $\alpha_\tau$  was usually free for larger  $|c_t|$  and  $(\sigma_h/\sigma_{h,\text{SM}})\text{Br}(h \rightarrow \mu\tau)$ , while  $|\alpha_t| \gtrsim 1$  were more favored for any case. While for case II in Table I, SuperB factory gave negative results but Super  $\tau$ -charm factory gave positive results,  $|\alpha_t| \lesssim 1$  would be favored, but for most cases there would be no constraints on  $\alpha_\tau$ .

FIG. 6:  $\text{Br}(\tau \rightarrow \mu\gamma)$  distributions in  $\alpha_t - \alpha_\tau$  plane for  $c_V = \Gamma_h/\Gamma_{h,\text{SM}} = 1$ , taking  $|c_t| = 1$  in the first line and  $|c_t| = 1.5$  in the second line, and  $(\sigma_h/\sigma_{h,\text{SM}})\text{Br}(h \rightarrow \mu\tau) = (1.5, 3, 6) \times 10^{-3}$  from left to right. The green regions are for  $\text{Br}(\tau \rightarrow \mu\gamma) < 2.4 \times 10^{-9}$ , the yellow regions are for  $2.4 \times 10^{-9} \leq \text{Br}(\tau \rightarrow \mu\gamma) < 5.4 \times 10^{-9}$ , the blue regions are for  $5.4 \times 10^{-9} \leq \text{Br}(\tau \rightarrow \mu\gamma) < 1 \times 10^{-8}$ , and the cyan regions are for  $\text{Br}(\tau \rightarrow \mu\gamma) \geq 1 \times 10^{-8}$ .



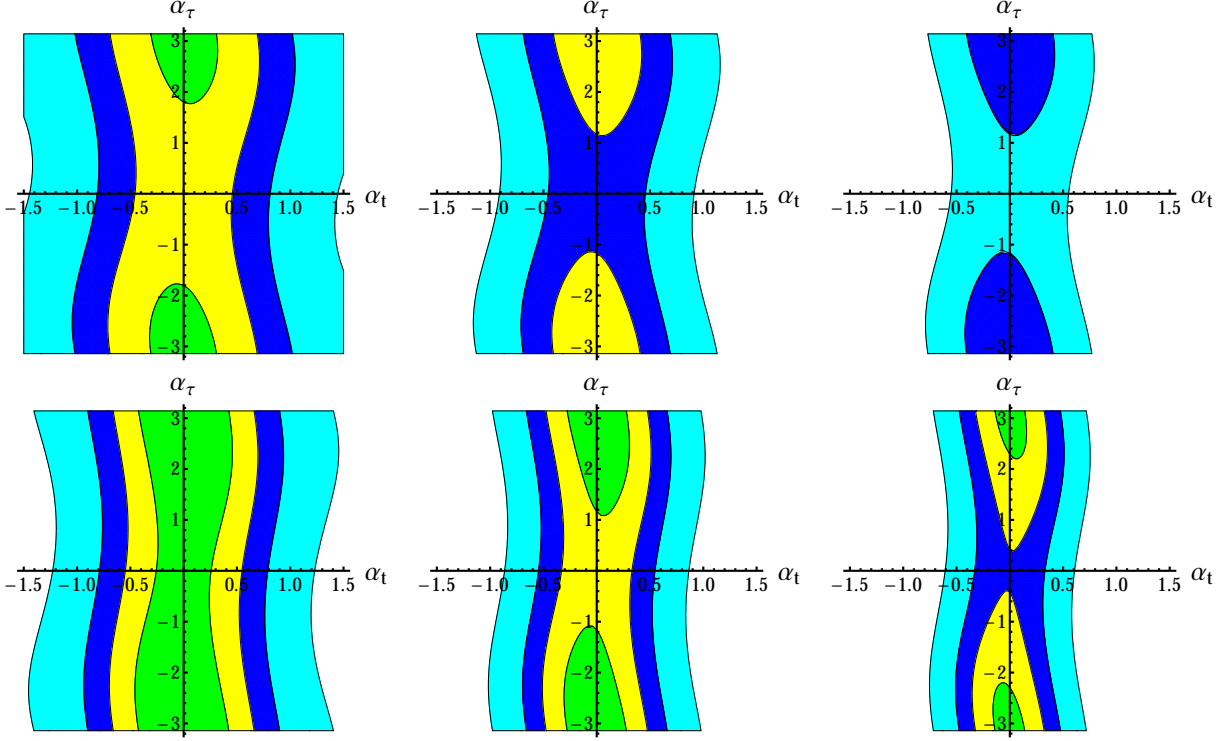
For case III in Table I that both factories gave negative results, larger  $|\alpha_\tau|$  and  $|c_t|$  would be favored.

Second, consider Lee model which is scenario II in section III. In this scenario, both  $c_V$  and  $\Gamma_h/\Gamma_{h,\text{SM}}$  are smaller than the predicted  $\text{Br}(\tau \rightarrow \mu\gamma)$  are smaller. For example, taking  $(\sigma_h/\sigma_{h,\text{SM}})\text{Br}(h \rightarrow \mu\tau) = 3 \times 10^{-3}$  as a benchmark point, the predicted  $\text{Br}(\tau \rightarrow \mu\gamma) \lesssim (0.8 - 1.6) \times 10^{-9}$  which cannot lead to a positive result at SuperB factory.

We show the  $\text{Br}(\tau \rightarrow \mu\gamma)$  distributions in  $\alpha_t - \alpha_\tau$  plane in Figure 8 with the boundaries set according to the sensitivity of Super  $\tau$ -charm factory, and all the colored regions are for  $\text{Br}(\tau \rightarrow \mu\gamma) < 2.4 \times 10^{-9}$ , thus case I in Table I would be disfavored.

In this scenario, the results for  $\text{Br}(\tau \rightarrow \mu\gamma)$  cannot reach the sensitivity of SuperB factory but they will reach the sensitivity of Super  $\tau$ -charm factory. If Super  $\tau$ -charm factory gave negative results as case III in Table I, it would give strict constraints on the Higgs couplings

FIG. 7:  $\text{Br}(\tau \rightarrow \mu\gamma)$  distributions in  $\alpha_t - \alpha_\tau$  plane for  $c_V = \Gamma_h/\Gamma_{h,\text{SM}} = 1$ , taking  $|c_t| = 1$  in the first line and  $|c_t| = 1.5$  in the second line, and  $(\sigma_h/\sigma_{h,\text{SM}})\text{Br}(h \rightarrow \mu\tau) = (1.5, 3, 6) \times 10^{-3}$  from left to right. The green regions are for  $\text{Br}(\tau \rightarrow \mu\gamma) < 2 \times 10^{-10}$ , the yellow regions are for  $2 \times 10^{-10} \leq \text{Br}(\tau \rightarrow \mu\gamma) < 5 \times 10^{-10}$ , the blue regions are for  $5 \times 10^{-10} \leq \text{Br}(\tau \rightarrow \mu\gamma) < 10^{-9}$ , and the cyan regions are for  $10^{-9} \leq \text{Br}(\tau \rightarrow \mu\gamma) < 2.4 \times 10^{-9}$ .



as well that  $|\alpha_t| \lesssim 1$  would be favored but the constraints on  $\alpha_\tau$  would be weak. While if Super  $\tau$ -charm factory gave positive results as case II in Table I, larger  $|c_t|$  and  $\alpha_t$  would be favored.

## B. LHC with Negative Result

In this subsection we choose  $(\sigma_h/\sigma_{h,\text{SM}})\text{Br}(h \rightarrow \mu\tau) = 7.7 \times 10^{-4}$  as the LHC expected 95% C.L. upper limit together with the replacement (16). In scenario I in section III where the coupling strengths are close to those in SM, the predicted  $\text{Br}(\tau \rightarrow \mu\gamma) \lesssim (1-2) \times 10^{-9}$ ; while in scenario II in section III, as the Lee model scenario, the predicted  $\text{Br}(\tau \rightarrow \mu\gamma) \lesssim (2-4) \times 10^{-10}$ .

We should discuss the two scenarios separately. We show the  $\text{Br}(\tau \rightarrow \mu\gamma)$  distributions

FIG. 8:  $\text{Br}(\tau \rightarrow \mu\gamma)$  distributions in  $\alpha_t - \alpha_\tau$  plane for  $c_V = 0.5$  and  $\Gamma_h/\Gamma_{h,\text{SM}} = 0.3$ , taking  $|c_t| = 0.8$  in the first line and  $|c_t| = 1.2$  in the second line, and  $(\sigma_h/\sigma_{h,\text{SM}})\text{Br}(h \rightarrow \mu\tau) = (1.5, 3, 6) \times 10^{-3}$  from left to right. The green regions are for  $\text{Br}(\tau \rightarrow \mu\gamma) < 2 \times 10^{-10}$ , the yellow regions are for  $2 \times 10^{-10} \leq \text{Br}(\tau \rightarrow \mu\gamma) < 5 \times 10^{-10}$ , the blue regions are for  $5 \times 10^{-10} \leq \text{Br}(\tau \rightarrow \mu\gamma) < 10^{-9}$ , and the cyan regions are for  $10^{-9} \leq \text{Br}(\tau \rightarrow \mu\gamma) < 2.4 \times 10^{-9}$ .

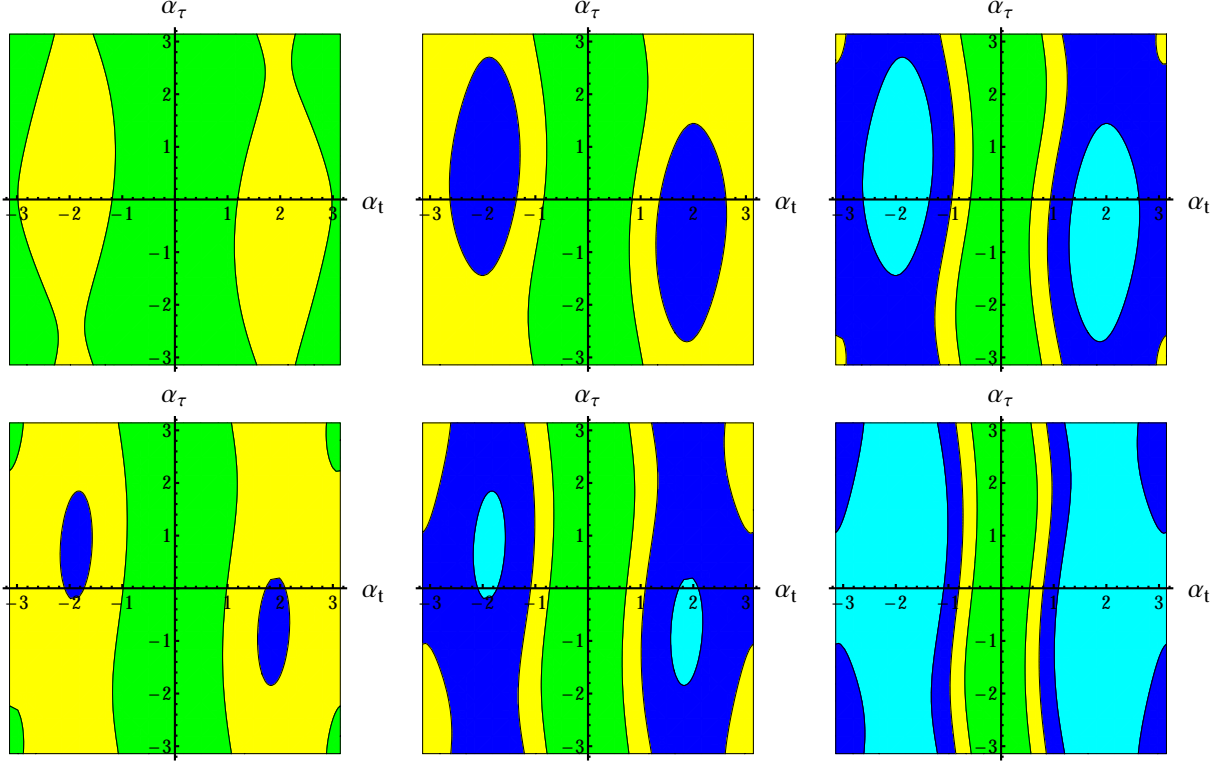


FIG. 9:  $\text{Br}(\tau \rightarrow \mu\gamma)$  distributions in  $\alpha_t - \alpha_\tau$  plane for  $c_V = \Gamma_h/\Gamma_{h,\text{SM}} = 1$ , taking  $|c_t| = 1, 1.2, 1.5$  from left to right. The green regions are for  $\text{Br}(\tau \rightarrow \mu\gamma) < 2 \times 10^{-10}$ , the yellow regions are for  $2 \times 10^{-10} \leq \text{Br}(\tau \rightarrow \mu\gamma) < 5 \times 10^{-10}$ , the blue regions are for  $5 \times 10^{-10} \leq \text{Br}(\tau \rightarrow \mu\gamma) < 10^{-9}$ , and the cyan regions are for  $10^{-9} \leq \text{Br}(\tau \rightarrow \mu\gamma) < 2.4 \times 10^{-9}$ .

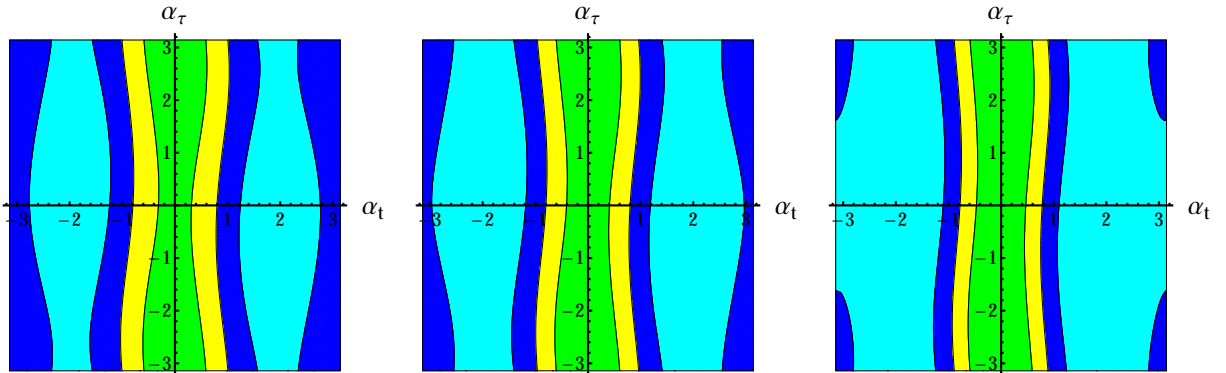
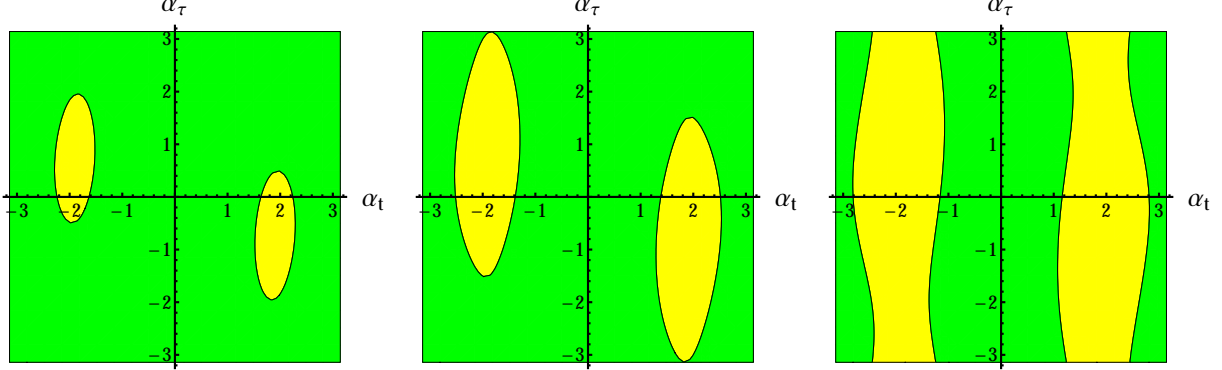


FIG. 10:  $\text{Br}(\tau \rightarrow \mu\gamma)$  distributions in  $\alpha_t - \alpha_\tau$  plane for  $c_V = 0.5$  and  $\Gamma_h/\Gamma_{h,\text{SM}} = 0.3$ , taking  $|c_t| = 1, 1.2, 1.5$  from left to right. The green regions are for  $\text{Br}(\tau \rightarrow \mu\gamma) < 2 \times 10^{-10}$ , the yellow regions are for  $2 \times 10^{-10} \leq \text{Br}(\tau \rightarrow \mu\gamma) < 5 \times 10^{-10}$ .



in  $\alpha_t - \alpha_\tau$  plane in Figure 9 for scenario I and in Figure 10 for scenario II respectively. If LHC gave negative results, the case I in Table I cannot appear thus we focus on case II and III. For scenario I, if Super  $\tau$ -charm factory gave negative results,  $|\alpha_t| \lesssim (0.3 - 1)$  would be favored, else the other regions would be favored. For scenario II, most regions are allowed for case III in Table I that both  $e^+e^-$  colliders gave negative results.

## V. CONCLUSIONS AND DISCUSSIONS

In this paper we discussed the Higgs- $\mu$ - $\tau$  coupling induced LFV decay processes  $h \rightarrow \mu\tau$  and  $\tau \rightarrow \mu\gamma$ . For the later process, the branching ratio is also closely related to the  $h\bar{t}t$ ,  $h\tau^+\tau^-$  and  $hW^+W^-$  couplings. We categorized the BSM into two scenarios, namely scenario I (II) with the Higgs coupling strengths close to (far away from) those in the SM, and for the latter scenario we took the Lee model as an example. We showed the possible numerical values of  $\text{Br}(\tau \rightarrow \mu\gamma)$  for different cases from Figure 4 to Figure 10.

If the future LHC run gives positive results on  $h \rightarrow \mu\tau$ , different measurements on  $\text{Br}(\tau \rightarrow \mu\gamma)$  at super B factory and super  $\tau$ -charm factory would distinguish the two scenarios or imply the favored parameter choices. For case I in Table I, with positive results from both SuperB and Super  $\tau$ -charm factories, scenario I would be favored while scenario II would be disfavored or even excluded. For typical parameter choices, see the blue or cyan regions in Figure 6 in details. For case II in Table I, with negative result from SuperB factory but positive result from Super  $\tau$ -charm factory, both scenarios would be allowed and some

constraints would be given on the Higgs couplings. See blue and cyan regions in Figure 7 and Figure 8 for scenario I and II separately to find detail information on parameter choices. For scenario I,  $\alpha_\tau$  would be free for most cases, but regions near  $(\alpha_t, \alpha_\tau) = (0, \pm\pi)$  would be disfavored for larger  $|c_t|$  and  $\text{Br}(h \rightarrow \mu\tau)$ . For scenario II,  $|\alpha_t| \gtrsim 1$  would be favored thus it implies large CP-violation in  $ht\bar{t}$  coupling. For case III in Table I, with negative results from both SuperB and Super  $\tau$ -charm factories, scenario II would be more favored, but scenario I would not be excluded. See green regions in Figure 7 and Figure 8 for scenario I and II separately.

If the future LHC run gives negative results on  $h \rightarrow \mu\tau$ , case I in Table I cannot be explained. If case I really happened, we would need other models. For case II in Table I, scenario I with  $|\alpha_t| \gtrsim (0.5 - 1)$  would be favored, which implies large CP-violation in  $ht\bar{t}$  coupling. While there would be almost no constraints on  $\alpha_\tau$ . See Figure 9 for details. For case III in Table I, nothing about LFV are to be seen at future colliders. Scenario I with  $|c_t| \gtrsim (0.5 - 1)$  would be excluded, while other regions for both scenarios are allowed.

In Table II we summarize the implications corresponded to all the six future possibilities depending on the measurements of  $\text{Br}(h \rightarrow \mu\tau)$  at the LHC and  $\text{Br}(\tau \rightarrow \mu\gamma)$  at the super B factory and super tau charm factories. With the help of future measurements on LFV processes  $h \rightarrow \mu\tau$  and  $\tau \rightarrow \mu\gamma$  at both high and low energy colliders, for most cases, we would be able to distinguish different BSM scenarios or set constraints on Higgs couplings. P-IV in Table II would be strange. If it is really the case in the future, the Higgs induced LFV would not be the underlying reason. It would require other mechanism beyond Higgs sector to generate large enough LFV processes such as  $\tau \rightarrow \mu\gamma$ .

### Acknowledgement

We thank Gang Li, Yuji Omura and Chen Zhang for helpful discussions. This work was supported in part by the Natural Science Foundation of China (Grants No. 11135003 and No. 11375014).

- 
- [1] N. Cabbibo, Phys. Rev. Lett. 10, 531 (1963); M. Kobayashi and T. Maskawa, Prog. Theor. Phys. 49, 652 (1973).

TABLE II: Short summary on all the future possibilities depending on the measurements  $\text{Br}(h \rightarrow \mu\tau)$  at the LHC and  $\text{Br}(\tau \rightarrow \mu\gamma)$  at the super B factory and super  $\tau$ -charm factories and their corresponding implications.

	$\text{Br}(h \rightarrow \mu\tau)$ @LHC	$\text{Br}(\tau \rightarrow \mu\gamma)$ @SuperB	$\text{Br}(\tau \rightarrow \mu\gamma)$ @Super $\tau$ -charm	Implications
P-I	Positive	Positive	Positive	Scenario I favored; Scenario II excluded.
P-II	Positive	Negative	Positive	Both scenarios allowed; Scenario I with small $ \alpha_t $ favored; Scenario II with large $ \alpha_t $ favored.
P-III	Positive	Negative	Negative	Scenario II more favored; Scenario I with small $ \alpha_t $ allowed.
P-IV	Negative	Positive	Positive	Cannot be explained here.
P-V	Negative	Negative	Positive	Scenario I with large $ \alpha_t $ favored; Scenario II disfavored.
P-VI	Negative	Negative	Negative	Scenario I with large $ \alpha_t $ disfavored; Other parameter regions allowed.

- [2] S. L. Glashow, J. Iliopoulos, and L. Maiani, Phys. Rev. D 2, 1285 (1970).
- [3] W. J. Marciano and A. I. Sanda, Phys. Lett. B 67, 303 (1977).
- [4] B. Pontecorvo, Zh. Eksp. Teor. Fiz. 33, 549 (1957) [Sov. Phys. JEPT 6, 429 (1957)]; Z. Maki, M. Nakagawa, and S. Sakata, Prog. Theor. Phys. 28, 870 (1962).
- [5] K. A. Olive et al. (Particle Data Group), Chin. Phys. C 38, 090001 (2014).
- [6] K. Hayasaka et. al. (Belle Collaboration), Phys. Lett. B 666, 16 (2008); B. Aubert et. al. (BaBar Collaboration), Phys. Rev. Lett. 104, 021802 (2010).
- [7] J. Adam et. al. (MEG Collaboration), Phys. Rev. Lett. 110, 201801 (2013).
- [8] J. Brodzicka et al. (Belle Collaboration), Prog. Theor. Exp. Phys. 04D001 (2012), arXiv: 1212.5342.
- [9] T. Aushev et. al., Report No. KEK Report 2009-12, arXiv: 1002.5012.
- [10] SuperB Collaboration, Report No. INFN/AE-10/2, LAL-110, SLAC-R-952, arXiv: 1008.1541.



- [11] A. M. Baldini et. al. (MEG Collaboration), arXiv: 1301.7225.
- [12] S.-H. Zhu, arXiv: 1410.2042.
- [13] ATLAS Collaboration, Phys. Lett. B 716, 1 (2012).
- [14] CMS Collaboration, Phys. Lett. B 716, 30 (2012).
- [15] M. Flechl (for the ATLAS and CMS Collaborations), arXiv: 1503.00632.
- [16] CMS Collaboration, Report No. CMS-HIG-14-005 and CERN-PH-EP-2015-027, arXiv: 1502.07400.
- [17] ATLAS Collaboration, Report No. CERN-PH-EP-2015-184, arXiv: 1508.03372.
- [18] G. C. Branco, P. M. Ferreira, L. Lavoura, M. N. Rebelo, M. Sher, and J. P. Silva, Phys. Rep. 516, 1 (2012).
- [19] J. D. Bjorken and S. Weinberg, Phys. Rev. Lett. 38, 622 (1977).
- [20] D. Aristizabal Sierra and A. Vicente, Phys. Rev. D 90, 115004 (2014).
- [21] D. Das and A. Kundu, Phys. Rev. D 92, 015009 (2015).
- [22] F. J. Botella, G. C. Branco, M. Nebot, and M. N. Rebelo, Report No. IFIC-15-62, arXiv: 1508.05101.
- [23] J. Heeck, M. Holthausen, W. Rodejohann and Y. Shimizu, Nucl. Phys. B 896, 281 (2015).
- [24] A. Crivellin, G. D'Ambrosio and J. Heeck, Phys. Rev. Lett. 114, 151801 (2015).
- [25] A. Crivellin, G. D'Ambrosio and J. Heeck, Phys. Rev. D 91, 075006 (2015).
- [26] Y.-N. Mao and S.-H. Zhu, Phys. Rev. D 90, 115024 (2014), arXiv: 1409.6844.
- [27] T. D. Lee, Phys. Rev. D 8, 1226 (1973).
- [28] L. de Lima, C. S. Machado, R. D. Matheus, L. A. F. do Prado, JHEP 1511, 074 (2015).
- [29] I. Doršner, S. Fajfer, A. Greljo, J. F. Kamenik, N. Košnik, and I. Nišandžić, JHEP 1506, 108 (2015).
- [30] K. Cheung, W.-Y. Keung, P.-Y. Tseng, arXiv: 1508.01897.
- [31] B. Bhattacharjee, S. Chakraborty, and S. Mukherjee, arXiv: 1505.02688.
- [32] Y. Omura, E. Senaha, and K. Tobe, JHEP 05, 028 (2015), arXiv: 1502.07824.
- [33] G. Blankenburg, J. Ellis, and G. Isidori, Phys. Lett. B 712, 386 (2012).
- [34] R. Harnik, J. Kopp, and J. Zupan, JHEP 03, 026 (2013).
- [35] C.-J. Lee and J. Tandean, JHEP 04, 174 (2015).
- [36] T. P. Cheng and M. Sher, Phys. Rev. D 35, 3484 (1987).
- [37] E. Levichev, Phys. Part. Nucl. Lett. 5, 554 (2008).

- [38] A. V. Bobrov and A. E. Bondar, Nucl. Phys. B (Proc. Suppl.) 253-255, 199 (2014).
- [39] J. P. Ma and C. H. Chang, Sci. China (Phys., Mech. and Astro.) 53, 1947-1948 (2010).
- [40] The LHC Higgs Cross Section Working Group, Report No. CERN-2013-004, arXiv: 1307.1347.
- [41] S. M. Barr and A. Zee, Phys. Rev. Lett. 65, 21 (1990); 65, 2920 (1990).
- [42] S. Davidson and G. Grenier, Phys. Rev. D 81, 095016 (2010).
- [43] D. Chang, W.-S. Hou, and W.-Y. Keung, Phys. Rev. D 48, 217 (1993).
- [44] J. Kopp and M. Nardecchia, JHEP 1410, 156 (2014), arXiv: 1406.5303.